Miloslav Vlasák; Jan Lamač

Save our stones – hysteresis phenomenon in porous media

In: Jan Chleboun and Pavel Kůs and Petr Přikryl and Miroslav Rozložník and Karel Segeth and Jakub Šístek (eds.): Programs and Algorithms of Numerical Mathematics, Proceedings of Seminar. Hejnice, June 21-26, 2020. Institute of Mathematics CAS, Prague, 2021. pp. 159–167.

Persistent URL: http://dml.cz/dmlcz/703111

Programs and Algorithms of Numerical Mathematics 20
J. Chleboun, P. Kůs, P. Přikryl, M. Rozložník, K. Segeth, J. Šístek (Eds.)
Institute of Mathematics of the Czech Academy of Sciences, Prague 2021

SAVE OUR STONES – HYSTERESIS PHENOMENON IN POROUS MEDIA

Miloslav Vlasák, Jan Lamač

Czech Technical University, Faculty of Civil Engineering
Thakurova 7, 166 29 Prague 6, Czech Republic
vlasamil@cvut.cz, lamacjan@cvut.cz

Abstract: We present a mathematical description of wetting and drying stone pores, where the resulting mathematical model contains hysteresis operators. We describe these hysteresis operators and present a numerical solution for a simplified problem.

Keywords: hysteresis, Preisach operator, porous media flow

MSC: 65M60, 74N30, 76S05

1. Introduction

Stone monuments, either stone statues as well as stone buildings, are endangered by corroding processes. To slow down these processes, it is possible to inject calcium hydroxide into the stone object, where it reacts with the carbon dioxide contained in the pores producing small limestone grains

$$\mathrm{Ca(OH)_2} + \mathrm{CO_2} \to \mathrm{CaCO_3} + \mathrm{H_2O}. \tag{1}$$

These limestone grains inside the pores improve the resistance of the stone objects to corroding processes.

Nevertheless, it is a very difficult task to manage the wetting and drying of the stone object correctly to obtain uniform distribution of limestone grains. To this end, there is a strong demand on the numerical modeling of this problem. Moreover, the process of pores wetting and drying exhibits hysteresis behavior. The aim of this paper is to briefly describe the mathematical model (for the more detailed description see [1], [4] and the citations therein), briefly introduce hysteresis operators involved in the problem and present a numerical solution for a simplified problem.

2. Balance laws

This section is based on [1]. Let us consider a time interval $(0, T)$ and a domain $\Omega \subset \mathbb{R}^3$ containing a solid deformable material with pores that contain a mixture

DOI: 10.21136/panm.2020.16

of liquid and gas. We describe the balance laws in the Lagrangean setting for the following state variables: u – the displacement vector, $\epsilon = \nabla_s u$ – the strain tensor, σ – the stress tensor, p – the capillary pressure, θ – the temperature, W – the relative liquid content, A – the relative gas content, C_S – the relative solid content ($1 - C_S$ is the porosity).

Let us assume the control volume $V_0 = V(0) \subset \Omega$. Then

$$V(t) = \{y \colon y = x + u(x,t), x \in V_0\}. \tag{2}$$

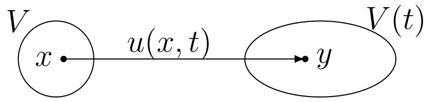

Figure 1: Evolution of the control volume.

We assume that the relative solid content is constant

$$\lim_{|V_0| \to 0,\, x \in V_0} \frac{|V_S(t)|}{|V_0|} = C_S \tag{3}$$

and the relative liquid and gas contents are

$$\lim_{|V_0| \to 0,\, x \in V_0} \frac{|V_W(t)|}{|V_0|} = W(x,t), \qquad \lim_{|V_0| \to 0,\, x \in V_0} \frac{|V_A(t)|}{|V_0|} = A(x,t), \tag{4}$$

respectively. Moreover, assuming small deformations we gain

$$\lim_{|V_0| \to 0,\, x \in V_0} \frac{|V(t)|}{|V_0|} \approx 1 + \operatorname{div} u(x,t). \tag{5}$$

From this immediately follows

$$A + W \approx 1 - C_S + \operatorname{div} u. \tag{6}$$

2.1. Mass balance

Following the empirical observations, we have a constitutive relation for the gas content A

$$A = G[p], \tag{7}$$

where $G[p]$ is the hysteresis operator. Let us assume that the liquid flux has the form

$$\xi = \mu(p) \nabla p, \tag{8}$$

where $\mu(p)$ is the permeability coefficient. We denote by ρ_L the liquid density. Then the mass balance reads

$$\frac{\mathrm{d}}{\mathrm{d}t}\int_V \rho_L W \mathrm{d}x + \int_{\partial V} \xi \cdot n \mathrm{d}s = 0. \tag{9}$$

From (6) and (9) we gain

$$\int_V \frac{\mathrm{d}}{\mathrm{d}t}(1 - C_S - G[p] + \operatorname{div} u) + \frac{1}{\rho_L}\operatorname{div}(\mu(p)\nabla p)\mathrm{d}x = 0 \tag{10}$$

for every control volume V. From this the differential relation

$$G[p]' - \operatorname{div} u' - \frac{1}{\rho_L}\operatorname{div}(\mu(p)\nabla p) = 0 \tag{11}$$

follows.

2.2. Momentum balance

The momentum balance for solids reads

$$\rho_S u'' = \operatorname{div}\sigma + g, \tag{12}$$

where ρ_S is the solid density, g represents volume forces (e.g. the gravity) and σ is given by an empirical constitutive relation

$$\sigma = B\epsilon' + P[\epsilon] + (p - \beta(\theta - \theta_C))\mathbf{1}, \tag{13}$$

where B is the constant symmetric positive definite tensor, β is the thermal expansion coefficient, θ_C is the reference temperature and P is the hysteresis operator describing elasto-plastic responds of solids. From (12) and (13) the differential relation

$$\rho_S u'' = \operatorname{div} B\epsilon' + \operatorname{div} P[\epsilon] + \nabla p - \beta\nabla\theta + g \tag{14}$$

follows.

2.3. Energy and entropy balance

Assuming Fourier's law

$$q = -\kappa\nabla\theta, \tag{15}$$

where κ is the heat conductivity constant and q is the heat flux. The first law of thermodynamics gives

$$U' + \operatorname{div} q = U' - \kappa\Delta\theta = \sigma : \epsilon' + \frac{1}{\rho_L}\operatorname{div}(p\mu(p)\nabla p), \tag{16}$$

where U is the energy density. The second law of thermodynamics gives

$$S' + \mathrm{div}\frac{q}{\theta} \geq 0, \tag{17}$$

where S is the entropy density. Let us assume that the hysteresis operators satisfy

$$P[\epsilon] : \epsilon' - V_P[\epsilon]' = \|D_P[\epsilon]'\|_*, \quad G[p]'p - V_G[p]' = |D_G[p]'|, \tag{18}$$

where V_P and V_G are the corresponding potential operators, D_P and D_G are the corresponding dissipation operators and $\|.\|_*$ is a seminorm. Moreover, setting the free energy

$$F = U - \theta S, \tag{19}$$

then according to (16) and (17) it is sufficient to satisfy

$$F' + \theta' S \leq \sigma : \epsilon' + \frac{1}{\rho_L}\mathrm{div}(p\mu(p)\nabla p). \tag{20}$$

It is possible to show that the relation (20) holds true for

$$F = V_p[\epsilon] + V_G[p] - \beta(\theta - \theta_C)\mathrm{div}\, u + F_0(\theta). \tag{21}$$

Assuming

$$F_0(\theta) = -c_0 \ln(\theta) + c_0 \ln(\theta_C), \tag{22}$$

we gain

$$c_0\theta' - \kappa\Delta\theta = \|D_P[\epsilon]'\|_* + |D_G[p]'| + B\nabla_s u' : \nabla_s u' + \frac{1}{\rho_L}\mu(p)|\nabla p|^2 - \beta\theta\mathrm{div}\, u'. \tag{23}$$

2.4. Solution existence for the isothermal case

Let us assume that the temperature θ remains constant, i.e. that there exist negative heat forces that prevent the temperature from changing. The complete system (11), (14), (23) simplifies to

$$\begin{aligned} G[p]' &= \mathrm{div}\, u' + \frac{1}{\rho_L}\mathrm{div}(\mu(p)\nabla p), \\ \rho_S u'' &= \mathrm{div} B\epsilon' + \mathrm{div} P[\epsilon] + \nabla p + g. \end{aligned} \tag{24}$$

We add the boundary conditions

$$u|_{\partial\Omega} = 0, \quad \mu(p)\nabla p \cdot n|_{\partial\Omega} = \gamma(x)(p^* - p), \tag{25}$$

where γ is the permeability of the domain's boundary and p^* is the outer pressure.

Assuming that the domain Ω is bounded with regular boundary, all the data are bounded and sufficiently regular, the hysteresis operator G satisfies $G[p] = G_0[p] + f(p)$, where G_0 is the Preisach operator and the function f is close to the function arctg, the hysteresis operator P satisfies $P[\epsilon] = A^e\epsilon + P_0[\epsilon]$, where A^e is a symmetric positive definite constant tensor and P_0 is a hysteresis operator satisfying certain continuity and balance relations, then it is possible to show that there exists a solution (u, p) of the problem (24). For more detailed description of the assumptions as well as for the complete proof see [1]. The uniqueness of the solution of the problem (24) remains open.

3. Hysteresis operators

The aim of this section is to describe some scalar hysteresis operators. For more detailed mathematical analysis of the hysteresis phenomenon see, e.g., [2] and [3].

3.1. Scalar Play operator

The Play operator is well known from mechanics, where this simple operator describes the delay in the response of mechanical parts. Let us assume the underlying function $p \in W^{1,1}(0,T)$ and the threshold $r > 0$. Then the Play operator $\mathfrak{p}_r \colon W^{1,1}(0,T) \to W^{1,1}(0,T)$ can be defined by the differential inequality

$$\begin{aligned} &|p(t) - \mathfrak{p}_r[p](t)| \le r \quad \forall t \in [0,T], \\ &\mathfrak{p}_r[p]'(t)(p(t) - \mathfrak{p}_r[p](t) - z) \ge 0 \quad \text{for a.e. } z \in [-r,r], \\ &\mathfrak{p}_r[p](0) \in [p(0) - r, p(0) + r]. \end{aligned} \tag{26}$$

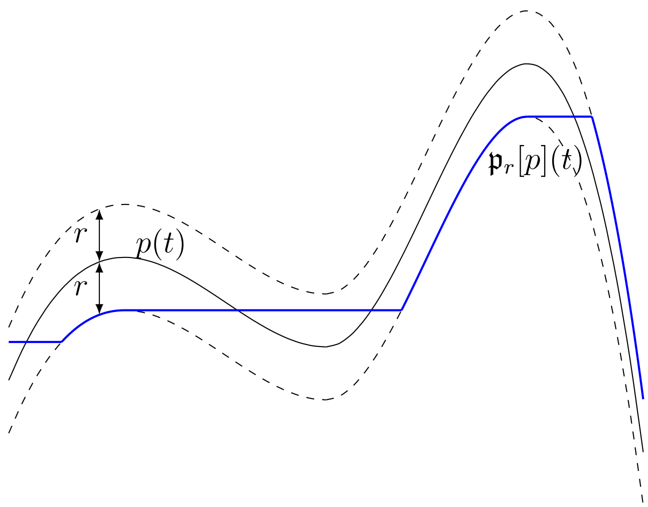

Figure 2: Application of the Play operator $\mathfrak{p}$ on given function p.

We can observe from Figure 2 that the Play operator works as the identity or it stagnates with the threshold given by r around the points of monotonicity change of the underlying function.

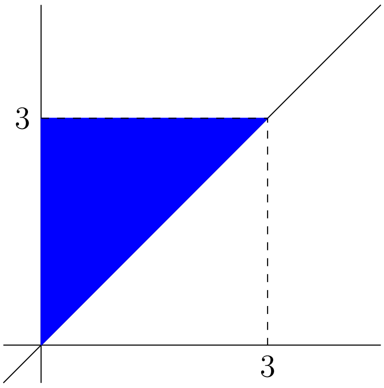

Figure 3: $G_0[p](t_1)$.

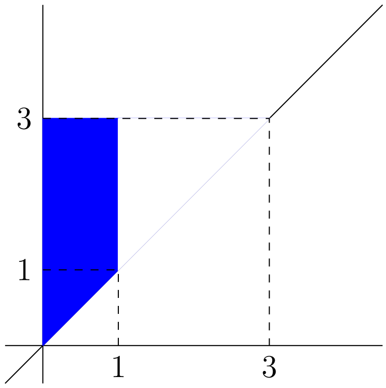

Figure 4: $G_0[p](t_2)$.

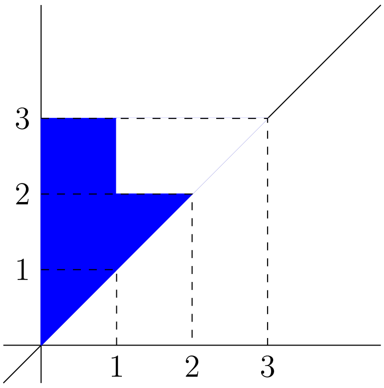

Figure 5: $G_0[p](t_3)$.

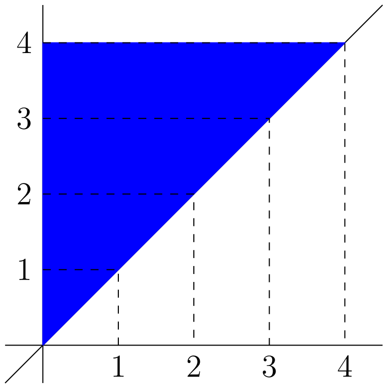

Figure 6: $G_0[p](t_4)$.

3.2. Preisach operator

The Preisach operator $G_0 : W^{1,1}(0,T) \to W^{1,1}(0,T)$ first described in [5] can be defined with the aid of Play operators by

$$G_0[p](t) = \int_0^\infty \int_0^{\mathfrak{p}_r[p](t)} \rho(r,s)\,\mathrm{d}s\,\mathrm{d}r, \tag{27}$$

where the function $\rho \in L^1((0,\infty)\times(-\infty,\infty))$ is the Preisach density. It is possible to describe this operator as a generalization of the sum of Play operators weighted by the density ρ. Let us define the transformation of the density $\hat{\rho}(\alpha,\beta) = \rho(r,s)$, where the transformation relation between (α,β) and (r,s) is

$$r = \frac{\beta-\alpha}{2}, \qquad s = \frac{\alpha+\beta}{2}. \tag{28}$$

Let us describe the evaluation of the Preisach operator on a simple example, where the underlying function p is piecewise monotone, increasing on the interval $[t_0,t_1]$ from 0 to 3, on the interval $[t_2,t_3]$ from 1 to 2 and on the interval $[t_3,t_4]$ from 2 to 4 and decreasing on the interval $[t_1, t_2]$ from 3 to 1, where $t_0 < t_1 < t_2 < t_3 < t_4$. For simplicity, let us assume that $G_0[p](t_0) = 0$. Then the value of $G_0[p](t_1)$ can be computed as the area of the right-angled triangle with the vertices $(0, 0)$, $(3, 3)$ and $(0, 3)$. The value of $G_0[p](t_2)$ can be computed by subtracting the area of the right-angled triangle with the vertices $(1, 1)$, $(3, 3)$ and $(1, 3)$ from $G_0[p](t_1)$. The value of $G_0[p](t_3)$ can be computed by adding the area of the right-angled triangle with the vertices $(1, 1)$, $(2, 2)$ and $(1, 2)$ to $G_0[p](t_2)$. And finally, the value of $G_0[p](t_4)$ can be computed as the area of the right-angled triangle with the vertices $(0, 0)$, $(4, 4)$ and $(0, 4)$. Moreover, all the areas are weighted by the density $\hat{\rho}$. For the illustration see Figures 3–6.

4. Numerical experiment

In this section we describe the numerical solution of the simplified problem to the system (11), (14), (23) mimicking the simplified system (24) analyzed in [1].

4.1. Problem setting

We assume the problem

$$\begin{aligned} \rho_S u'' + cu' &= \nu \Delta u + (\nu + \lambda)\nabla \operatorname{div} u + \nabla p, \\ G[p]' &= \operatorname{div} u' + \frac{\mu}{\rho_L}\Delta p \end{aligned} \tag{29}$$

with the boundary conditions

$$u|_{\partial\Omega} = 0, \quad \mu \nabla p \cdot n|_{\partial\Omega} = \gamma(1 - p) \tag{30}$$

and the initial conditions

$$\begin{aligned} u(x, 0) &= (\sin(\pi x_1)\sin(\pi x_2), 16x_1x_2(1 - x_1)(1 - x_2))^T, \\ u'(x, 0) &= (0, 0)^T, \\ p(x, 0) &= 1. \end{aligned} \tag{31}$$

We assume the domain is a unit square $\Omega = (0, 1)^2$, the time interval is $(0, 5)$ and

$$G[p] = G_0[p] + \operatorname{arctg}(p), \tag{32}$$

where G_0 is the Preisach operator described in Sec. 3.2. We assume that the parameters of the problem are chosen in the following way

$$\rho_S = \nu = \lambda = \mu = \rho_L = \gamma = 1, \quad c = 0. \tag{33}$$

4.2. Discretization

The space discretization is carried out with the aid of the classical finite element method on the uniform mesh with the mesh size $h = 0.025$, a piecewise linear approximation for the pressure p and a piecewise quadratic approximation for the displacement u. The resulting ODE system is discretized by the finite difference method with the uniform time step $\tau = 0.005$, where

$$u''(t) \approx \frac{u(t) - 2u(t-\tau) + u(t-2\tau)}{\tau^2}. \tag{34}$$

The implicit approximation of $u''(t)$ is only of the first order, but it improves the stability of the resulting scheme with respect to the choice of the step-size τ.

Moreover, it is necessary to discretize $G[p]'$ term. To achieve good stability properties with respect to the step-size τ and to avoid the solution of nonlinear problems, we apply a semi-implicit discretization. According to the assumption (32), we approximate

$$G[p]'(t) \approx \left(G_0'[p](t-\tau) + \frac{1}{p(t-\tau)^2 + 1} \right) \frac{p(t) - p(t-\tau)}{\tau}, \tag{35}$$

where $G_0'[p]$ represents the infinitesimal increment of the Preisach operator $G_0[p]$. With the aid of the ideas from Sec. 3.2, we can evaluate the value of $G_0'[p](t-\tau)$ as the length of the last line (weighted by the density $\hat{\rho}$) infinitesimally added to/subtracted from the final area for evaluation of $G_0[p](t-\tau)$, see Figures 3–6.

4.3. Results

The evolution of the capillary pressure p is displayed in Figures 7–12, where the higher values are in red and the lower values are in blue. It is possible to observe that the pressure p oscillates. This oscillation is much stronger in $(0,0)$ and $(1,1)$ corners. On the contrary, the solution p almost stagnates along the diagonal $x_1 + x_2 = 1$. Moreover, these oscillations are damped as time evolves. This is due to the strong damping properties of the Δp term in (29).

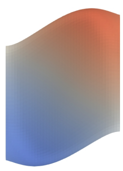

Figure 7: $p(t = 0.175)$.

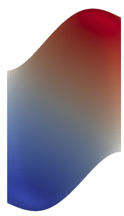

Figure 8: $p(t = 0.35)$.

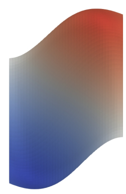

Figure 9: $p(t = 0.525)$.

We are interested in the evolution of the Preisach operator $G[p(0.9, 0.9)]$ in time, i.e., at the point $x = (0.9, 0.9)$, where p has large oscillations. The results are shown in Figure 13. The corresponding hysteresis loops, i.e., the dependence of the Preisach operator $G[p(0.9, 0.9)]$ on the value of $p(0.9, 0.9)$, are visualized in Figure 14.

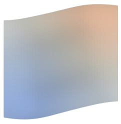

Figure 10: $p(t = 0.7)$.

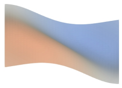

Figure 11: $p(t = 0.875)$.

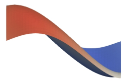

Figure 12: $p(t = 1.05)$.

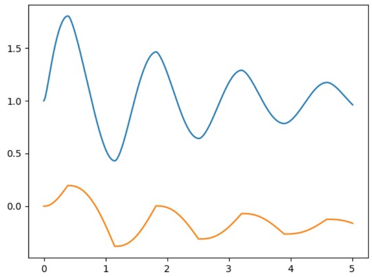

Figure 13: Evolution in time: $p(0.9, 0.9)$ – the upper curve, $G[p(0.9, 0.9)]$ – the lower curve.

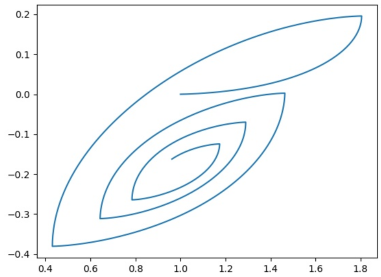

Figure 14: Dependence of $G[p(0.9, 0.9)]$ on $p(0.9, 0.9)$.

Acknowledgements

The research of Miloslav Vlasák was supported by Grant No. 20-14736S of the Czech Science Foundation. The research of Jan Lamač was supported by the European Regional Development Fund-Project "Center for Advanced Applied Science" (No. CZ.02.1.01/0.0/0.0/16 019/0000778).

References

[1] Albers, B. and Krejčí P.: Unsaturated porous media flow with thermomechanical interaction. Math. Methods Appl. Sci. **39**(9) (2016), 2220–2238.

[2] Brokate M. and Sprekels J.: *Hysteresis and phase transitions*. Appl. Math. Sci. **121**, NY: Springer, New York, 1996.

[3] Krasnosel'skij M. A. and Pokrovskij A. V.: *Systems with hysteresis. Transl. from the Russian by Marek Niezgódka*. Springer-Verlag, Berlin, 1989.

[4] Krejčí P., Rocca E., and Sprekels J.: Unsaturated deformable porous media flow with thermal phase transition. Math. Models Methods Appl. Sci. **27**(14) (2017), 2675–2710.

[5] Preisach F.: Über die magnetische Nachwirkung. Z. Phys. **94** (1935), 277–302.